Biomaterials Science

Intrinsically Semi-Permeable PDMS Nanosheet Encapsulating Adipose Tissue-Derived Stem Cells for Enhanced Angiogenesis

Journal:	*Biomaterials Science*
Manuscript ID	BM-ART-03-2024-000460
Article Type:	Paper
Date Submitted by the Author:	31-Mar-2024

Complete List of Authors:	Takuma, Megumi; Tokyo Institute of Technology, School of Life Science and Technology Fujita, Hajime; Tokyo Institute of Technology - Suzukakedai Campus, School of Life Science and Technology Zushi, Nanami; Tokyo Institute of Technology - Suzukakedai Campus, School of Life Science and Technology Nagano, Hisato; National Defense Medical College, Department of Plastic and Reconstructive Surgery Azuma, Ryuichi; National Defense Medical College, Department of Plastic and Reconstructive Surgery Kiyosawa, Tomoharu; National Defense Medical College, Department of Plastic and Reconstructive Surgery Fujie, Toshinori; Tokyo Institute of Technology, School of Life Science and Technology; Tokyo Institute of Technology, Living Systems Materialogy Research Group, International Research Frontiers Initiative

Biomaterials Science

Article

Intrinsically Semi-Permeable PDMS Nanosheet Encapsulating Adipose Tissue-Derived Stem Cells for Enhanced Angiogenesis

Received 00th January 20xx,
Accepted 00th January 20xx

DOI: 10.1039/x0xx00000x

Megumi Takuma[a], Hajime Fujita[a], Nanami Zushi[a], Hisato Nagano[b], Ryuichi Azuma[b], Tomoharu Kiyosawa[b], Toshinori Fujie*[a,c]

Cell encapsulation devices are expected to be promising tools that can control the release of therapeutic proteins secreted from transplanted cells. Protein permeability of the device membrane is important because it allows the isolation of transplanted cells while enabling the effectiveness of the device. In this study, we investigated free-standing polymeric ultra-thin films (nanosheets) as an intrinsically semi-permeable membrane made from polydimethylsiloxane (PDMS). The PDMS nanosheet with a thickness of 600 nm showed intrinsic protein permeability, and the device fabricated with the PDMS nanosheet showed that VEGF secreted from implanted adipose tissue-derived stem cells (ASCs) could be released for at least 5 days. The ASC encapsulation device promoted angiogenesis and the development of granulation tissue during 1 week after transplantation to the subcutaneous area of a mouse. This cell encapsulation device consisting of PDMS nanosheet provides a new method for pre-vascularization of the subcutaneous area in cell transplantation therapy.

1 Introduction

As a future avenue for drug delivery, cell encapsulation devices are promising tools that can control the release of therapeutic proteins secreted from transplanted cells; such devices would be a better delivery solution than the repeated injections currently needed for protein pharmaceuticals[1–6]. These devices should be implanted in subcutaneous tissue, which is a minimally invasive target, and would allow the removal of the graft if necessary[7,8]. However, the relatively sparse distribution of blood vessels in subcutaneous tissue might result in a lack of nutrients and the loss of the transplanted cells[7–11]. Therefore, pre-vascularization of the implantation site is required to promote the delivery of cell-derived therapeutic proteins (e.g., growth factors from stem cells, insulin from islet cells)[8,10,12–14]. In such cases, single cells or an aliquot of cells are encapsulated by a soft semi-permeable membrane to allow the transport of therapeutic proteins and nutrients.

There are two options for designing these soft semi-permeable membranes: 1) fabrication with micropores[15] (i.e., a mesh-like membrane or sheet-like membrane with track-etched holes) and 2) changing the thickness of a polymeric thin film[16]. The micropore fabrication technique has the advantage of creating a uniform pore size[17,18], but the micropores potentially allow the elution of culture medium from the device without molecular selectivity. In a previous study, we developed free-standing polymeric ultra-thin films (referred to as "nanosheets") as intrinsically semi-permeable membranes[16]. Permeability was endowed owing to the structural change formed by the crystallization of constituent polymers upon thermal treatment, which resulted in the selective permeation of molecules through cavities among the entangled polymer chains[16]. Such self-assembled cavities in the intrinsically semi-permeable membrane would prevent the spontaneous elution of liquid culture medium, overcoming the drawback of microfabricated porous membranes. Inspired by this finding, here, we explored the capabilities of intrinsically semi-permeable membranes for the prolonged release of cell-derived therapeutic proteins.

We selected polydimethylsiloxane (PDMS) from among candidate polymers as the most suitable material for fabricating a semi-permeable membrane because of its biocompatibility and flexibility in the form of a thin film[19], and its non-degradability for xenotransplantation. PDMS has been used to develop drug-releasing devices, such as the steroid-releasing Norplant[20,21]; however, Norplant's permeation membrane is only suitable for the sustained release of small molecules with a molecular weight of 312 Da, molecular weight of a therapeutic drug released from Norplant (levonorgestrel[20]). We also previously found that coating a precursor solution of PDMS diluted with a mixed organic solvent of *n*-hexane and ethyl acetate led to a decreased crosslinking degree of the PDMS nanosheet[19]. In those results, we also evaluated the influence of organic solvents on the crosslinking degree and on protein permeability through the PDMS nanosheet.

In the present study, we report the design of an intrinsically semi-permeable PDMS nanosheet, the fabrication of the PDMS nanosheet integrated into a cell encapsulation device, and the evaluation of *in vivo* preconditioning via the paracrine effect derived from the encapsulated stem cells as a proof-of-concept study in cell therapy (Fig. 1). Specifically, we investigated the semi-permeability of the

[a] *School of Life Science and Technology, Tokyo Institute of Technology, B-50, 4259 Nagatsuta-cho, Midori-ku, Yokohama 226-8501 (Japan).*
[b] *Department of Plastic and Reconstructive Surgery, National Defense Medical College, Tokorozawa, Saitama 359 8513 (Japan).*
[c] *Living Systems Materialogy Research Group, International Research Frontiers Initiative, Tokyo Institute of Technology, B-50, 4259 Nagatsuta-cho, Midori-ku, Yokohama 226-8501 (Japan).*
† Footnotes relating to the title and/or authors should appear here.
Electronic Supplementary Information (ESI) available: [details of any supplementary information available should be included here]. See DOI: 10.1039/x0xx00000x

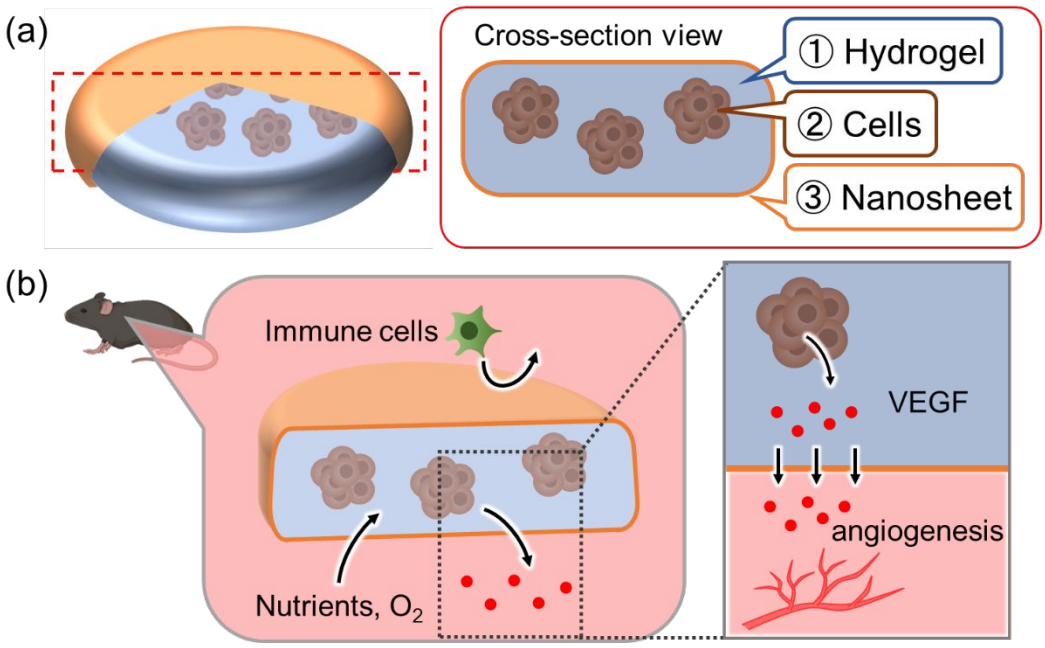

Fig. 1 Overview of the study. (a) Illustration of the cell encapsulation device consisting of hydrogel (GelMA), protein-secreting cells (ASCs), and an intrinsically semi-permeable PDMS nanosheet. (b) The PDMS nanosheet isolates encapsulated cells from the surrounding immune cells and allows the permeation of nutrients, oxygen, and proteins (e.g., VEGF) released from ASC spheroids.

therapeutic protein vascular endothelial growth factor (VEGF), which is known to give the angiogenesis effect[22], through the PDMS nanosheet. Then, we encapsulated spheroids of adipose tissue-derived stem cells (ASCs), VEGF secreting cells[22–24], within the PDMS nanosheets. We also investigated the ability of the ASC spheroid encapsulation device to release VEGF *in vitro*. Finally, we evaluated the angiogenic effect in terms of pre-vascularization induced by the implanted device *in vivo*. Our design and fabrication of the cell encapsulation device took advantage of polymeric nanosheets, and it achieved controlled permeability of therapeutic proteins with the good conformability to the transplanted site.

2 Materials and methods

Materials

Polydimethylsiloxane (PDMS) (SILPOT 184) was purchased from DuPont Toray Specialty Materials K.K. (Tokyo, Japan). Polyethylene terephthalate (PET) film (Lumirror T60) was purchased from Toray Industries, Inc. (Tokyo, Japan). Hexane, Dulbecco's phosphate-buffered saline (-) (PBS), 7.5 w/v% albumin D-PBS (-), and bovine serum albumin solution were purchased from Fujifilm Wako Pure Chemical Corporation (Osaka, Japan). Ethyl acetate and polyvinyl alcohol (PVA) (polymerization approximately 500 86.5%–89% hydrolyzed) was purchased from Kanto Chemical Co., Inc. (Tokyo, Japan). Gelatin methacrylate (GelMA, gel strength 300 g Bloom, 80% degree of substitution), Albumin-fluorescein isothiocyanate conjugate (FITC-BSA) (protein bovine), and 2-hydroxy-2-methyl-1-phenylpropanone (Irgacure 1173) were purchased from Sigma-Aldrich Co. Llc., (St. Louis, US). 2-Hydroxy-4'-(2-hydroxyethoxy)-2-methylpropiophenone (Irgacure 2959) and phenylbis(2,4,6-trimethylbenzoyl)phosphine oxide) (Irgacure 819) were purchased from Tokyo Chemical Industry Co., Ltd. (Tokyo, Japan). Low Cell Adhesion Products (PrimeSurface™) was purchased from Sumitomo Bakelite Co., Ltd. (Tokyo, Japan). Dulbecco's modified Eagle medium: Nutrient Mixture F-12 (DMEM/F12), fetal bovine serum, penicillin-streptomycin, and trypsin-EDTA were purchased from Thermo Fisher Scientific (Waltham, US). FITC-labeled mouse anti-Human IgG (H+L) Secondary Antibody (FITC-IgG) was purchased from Novus biological (Centennial, US).

Preparation of PDMS nanosheets

The PDMS nanosheets were fabricated on a PET film using gravure coating (ML-120, Yasui Seiki Co., Ltd., Tokyo, Japan) or bar coating (TC-1, Mitsui Electric Co., Ltd., Chiba, Japan) for the PDMS layer, and gravure coating for the PVA sacrificial layer. To prepare the sacrificial PVA layer, a PVA solution (10 wt%) was coated onto the PET film substrate at a line speed of 1.3 m min^{-1} and a gravure rotation speed of 30 rpm at 80°C. After the solvent was evaporated, pre-cured PDMS at a ratio of 10:1 (w/w) was coated onto the PVA/PET film. Film thicknesses of 300 nm, 600 nm, and 2.4 µm (which were used for the permeation test) were made from PDMS diluted in hexane: ethyl acetate (4:1 v/v) at concentrations of 30 wt%, 15 wt%, and 50 wt%, respectively; the rotation speed was 30, 30, and 50 rpm, respectively. For all concentrations, the line speed was 0.2 m min^{-1} and the drying temperature was 120°C. The 2 µm thickness used for the tensile test and FTIR, and the 4.8 µm thickness used for the permeation test, were fabricated by bar coating a pre-cured PDMS solution (without dilution) onto the PVA/PET film at a coating speed of 10 mm sec^{-1}. All PDMS sheets were baked in an oven at 120°C for 1.5 h followed by 80°C for 12 h to cure the PDMS layer.

PDMS nanosheet characterization

To observe the surface of the PDMS nanosheets, fabricated PDMS nanosheets were fixed on a pin stub and covered with gold using sputtering equipment (MSP-20-TK vacuum device, Ibaraki, Japan). The surface of the PDMS nanosheets was observed by SEM (ProX Phenom-World, JASCO Corporation, Tokyo, Japan). The FTIR

spectra were obtained using an FTIR spectrometer (ALPHA II, Bruker, Billerica, US). Tensile tests were conducted to evaluate the mechanical properties of the PDMS sheets (thickness: 2 µm, 100 µm) under dry and wet conditions using a tensile tester (EZ-SX, Shimadzu, Kyoto, Japan) (load cell: 5 N (2 µm wet) and 100 N (2 µm dry and 100 µm). Dried sheets were prepared by removing the PVA layer by soaking in water for 10 min, rinsing with pure water, and then air-drying for several hours. Wet sheets were prepared by soaking the sheets in water for several hours after the PVA layer was removed.

Evaluation of protein permeability through the PDMS nanosheet

Transwell prefixed membranes (ThinCert, Greiner, Kremsm ü nster, Austria) were removed and replaced with PDMS nanosheets with thicknesses of 300 nm, 600 nm, 2.4 µm, or 4.8 µm. Each modified Transwell was then placed in an individual well of a 24-well microplate. PBS was added to the outer well, and BSA (9.4 mg mL^{-1}), as a model protein, was added to the inner well. The amount of BSA in the outer well was monitored using a Bradford protein assay kit (23200, Thermo Scientific) and a multiple plate reader (EnSPire 2300-00J, PerkinElmer, Waltham, US) over a 24 h period. Similarly, the permeability of FITC-labeled BSA and FITC-labeled IgG (5 µM each) was evaluated using Transwell replaced with PDMS nanosheet with thickness of 800 nm fixed with adhesive (BONDIC, EIGERTOOL). The amount of FITC-labeled BSA and FITC-labeled IgG in the outer solution was monitored respectively and quantified by a multiple plate reader.

Preparation and characterization of GelMA

Irgacure 2959 was dissolved in PBS at a concentration of 0.5% (w/v) in the dark. GelMA was dissolved at a concentration of 5% (w/v) in the Irgacure 2959 solution in the dark at 37°C. To evaluate the mechanical properties of crosslinked GelMA (1,000 mJ cm^{-2}), a compression test was conducted using a texture analyzer (TA-100/650E: TA.XT Plus 100C, Eko Instruments Co., Ltd., Tokyo, Japan) (jig: P/6, compression speed: 0.5 mm sec^{-1}, compressive modulus: 60%, trigger weight: 0.1 g, load cell: 500 g).

Cell culture and formation of ASC spheroids

Adipose tissue-derived stem cells (ASCs) from C57BL/6 mice (Cyagen Biosciences Inc., Santa Clara, US) were cultured in growth medium (Dulbecco's modified Eagle medium: Nutrient Mixture F-12 (DMEM/F12), 10% (v/v) fetal bovine serum, and 1% (v/v) penicillin-streptomycin) in a 5% CO_2 atmosphere at 37°C. When the cells reached 80%–90% confluency, they were detached from the cell culture flask with 0.25% (w/v) trypsin-EDTA. ASC spheroids were generated by seeding a suspension of ASCs into each well of a low-adherent 96-well microplate (PrimeSurface) at a seeding density of 500 cells per well. To evaluate the viability of the cells within the ASC spheroids, a live/dead viability assay (Live/Dead Cell Staining Kit II, TaKaRa, Shiga, Japan) was performed. After 30–60 min of incubation, the distribution of live cells was observed with a fluorescence microscope (BZ-X700, Keyence, Osaka, Japan).

Encapsulation of ASC spheroids in GelMA

ASC spheroids in growth medium were collected after 24 h of incubation in a 5% CO_2 atmosphere at 37°C. The supernatant was removed after centrifugation, and 5% (w/v) GelMA/Irgacure 2959 solution in growth medium, which was sterilized with a 0.22 µm filter, was added to the spheroid pellet at a concentration of 3 µL/spheroid and resuspended. Aliquots (150 µL) of spheroid/GelMA solution were pipetted into a 48-well microplate and photo-crosslinked under different UV irradiation energies with a UV crosslinker (CL-1000, 365 nm, Analytik Jena, Jena, Germany). After cross-linking, the encapsulated spheroids were cultured for 1 day.

Fabrication of cell encapsulation device for *in vitro* experiment

ASC spheroids were formed by seeding 500 ASCs into each well of a PrimeSurface plate. Within 24 h of seeding, the ASCs had formed spheroids. The spheroids were collected and resuspended in 5% (w/v) GelMA in DMEM/F12 medium. Next, a PDMS sheet was fixed onto a glass plate, and 5% (w/v) GelMA solution in PBS (photo initiator (PI): Irgacure 819, 1173) was poured onto the sheet. The material was then photocrosslinked by placing it under a blue laser equipped with SPACE ART (Kantatsu, Tokyo, Japan) for 3 min to fabricate the donut-shaped frame. After removing the uncrosslinked GelMA, 50 µL of the 1,000 spheroid suspension in 5% (w/v) GelMA in DMEM/F12 medium (PI: Irgacure 2959) was dispensed inside the frame, and UV light (1,000 mJ cm^{-2}) was irradiated to crosslink the GelMA surrounding the ASC spheroids. After cross-linking, a PDMS nanosheet (thickness: 600 nm) was overlaid to encapsulate the GelMA and spheroids, and the device was obtained by laser cutting around the GelMA-based frame.

Evaluation of VEGF secretion from ASC spheroids

After culturing the ASC spheroids for 1 day in a non-crosslinked GelMA solution, PBS was added to each well, and the spheroids were further incubated for 3 hours in a 5% CO_2 atmosphere at 37°C to diffuse the secreted protein. The supernatant was then analyzed by ELISA to determine the amount of secreted VEGF. Additionally, the cell encapsulation device was soaked in culture medium, and the medium was collected daily for 5 days. The amount of VEGF was measured using a sandwich ELISA kit (VEGF-A Mouse ELISA Kit (BMS619-2, Invitrogen, Waltham, US).

Fabrication of ASC spheroid encapsulation device for *in vivo* experiment

The fabrication process of an *in vivo* cell encapsulation device, particularly the preparation of the donut-shaped frame made from GelMA, was modified from the process used to fabricate the *in vitro* cell encapsulation device. This made the entire process simple and clean, and could be easily adapted for the animal experiments. To fabricate the donut-shaped frame, a mold was printed by a 3D gel printer (BIO X, CELLINK, Gothenburg, Sweden) instead of directly fabricating the frame by crosslinking the GelMA with the blue laser of the stereo lithography apparatus (SLA) printer. The mold was made by forming water-soluble gelink (CELLINKSTART, CELLINK) into two donut rings with different diameters to make a ring-shaped interspace (outer diameter: 10 mm, inner diameter: 8.4 mm, height: 1 mm). The GelMA-based donut-shaped frame was then fabricated by injecting a 10% (w/v) GelMA solution (PI: 0.5% (w/v) Irgacure 2959) and crosslinking under UV light (365 nm, 1 min). The water-soluble gel ink was then rinsed away. Next, the fabricated donut-shaped frame was fixed onto PDMS sheets with thicknesses of 2–10 µm, and 50 µL of ASC spheroids suspended in GelMA solution was dispensed into the frame. After 1 min of UV (365 nm) exposure, the PDMS nanosheet with a thickness of approximately 600 nm was

overlaid on the GelMA and dried in air for approximately 20 min to allow attachment. The PDMS nanosheet was then cut in a circle with a diameter of approximately 15 mm to obtain the device, which was placed on a mesh to keep it safe until the transplantation.

Preparation of ASC spheroids for *in vivo* evaluation of angiogenic effect

A suspension of ASCs was seeded into each well of a PrimeSurface 384-well plate at a density of 10^3 cells/well with 30 µL of growth medium per well. The cells were incubated in a 5% CO_2 atmosphere at 37°C for 1 day to form spheroids. The ASC spheroids were then removed to a centrifuge tube by gentle pipetting, and the supernatant was removed. Next, the ASC spheroids were resuspended in 5% (w/v) GelMA to prepare the ASC spheroid–GelMA suspension. In detail, the GelMA solution was added at a density of 4×10^3 spheroids mL^{-1} for encapsulating 2,000 spheroids in one device. After preparing the cell encapsulation device with 2,000 spheroids, additional GelMA solution was added to adjust the final concentration to 200 spheroids mL^{-1}.

Subcutaneous transplantation of cell encapsulation device and evaluation of angiogenic effect

C57BL/6 mice (male, 8–12 weeks old, 25–30 g; Japan SLC Inc., Shizuoka, Japan) were used for animal experiments. All animal procedures were performed in accordance with the Guidelines for Care and Use of Laboratory Animals of the National Defense Medical College, and approved by the Animal Ethics Committee of the National Defense Medical College (permission number: 22021).

The subcutaneous transplantation area was prepared by incising the median line in the back and removing the skin from the muscular coat to prepare a space to transplant the device into the right flank region. The transplantation region was exposed to the air by removing the skin with scissors. The cell encapsulation device was placed in the exposed transplantation region, the skin was replaced, and the incision line was sutured. On Day 7, a histological examination was performed by preparing specimens from each mouse The device with skin and fascia was fixed in 10% formaldehyde and stained with HE and CD31 to examine the area for capillary vessels. After embedding in a paraffin block, the specimens were sliced and observed under an optical microscope. The area with blood vessels was analyzed using ImageJ.

Statistical analyses

Statistical analysis was performed using one-way ANOVA and Bonferroni's multiple comparison test.

3 Results and Discussion

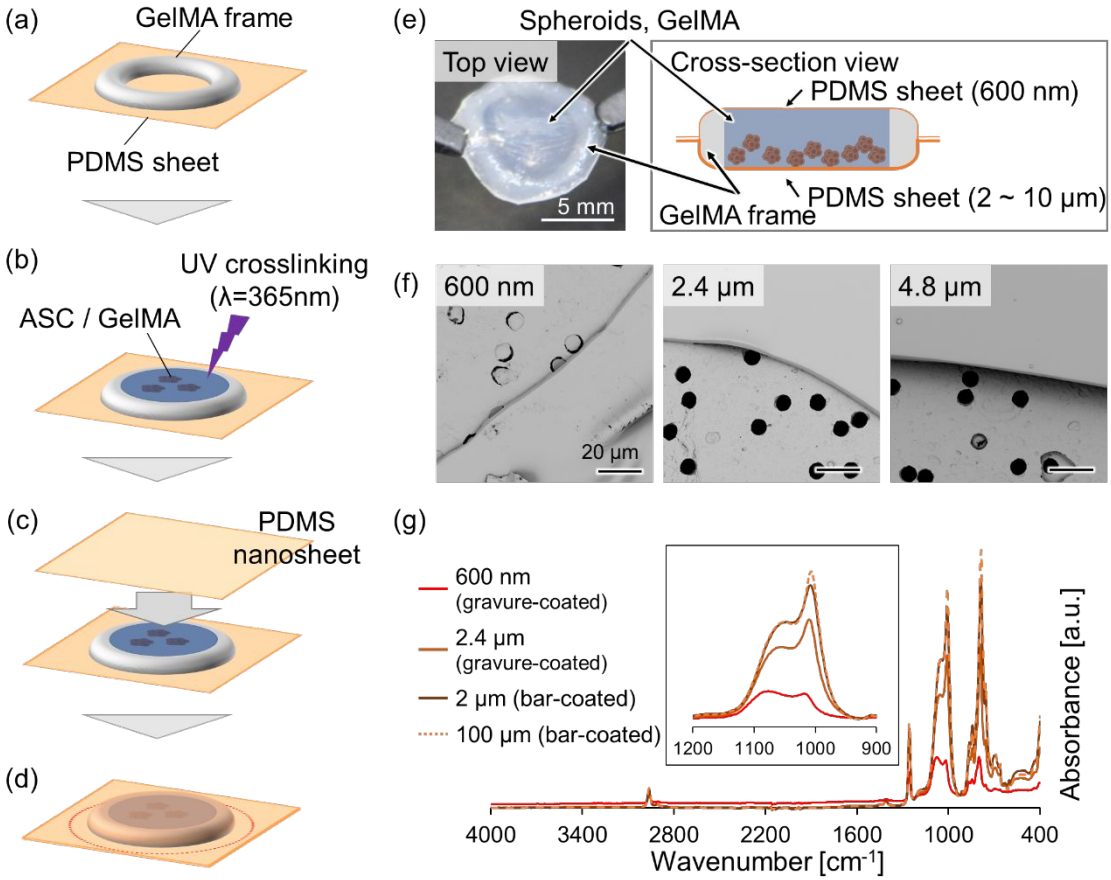

Fig. 2 Fabrication of ASC spheroid–hydrogel composite encapsulated by a nanosheet. (a) Fabrication of a GelMA-based frame on PDMS sheet. (b) Injection of spheroid suspension into GelMA. (c) Sandwiching with PDMS nanosheet. (d) Removal of excess PDMS sheet to obtain the device. (e) Optical image of the top view and an illustration of the cross-sectional view of the device. (f) SEM image of PDMS nanosheet (thickness: 600 nm, 2.4 µm, 4.8 µm) on a filter membrane with a pore size of 8.0 µm in diameter. (g) IR spectra of PDMS nanosheets with different thicknesses (red: 600 nm by gravure coating; light brown: 2.4 µm by bar coating; brown: 2 µm by gravure coating; orange dotted line: 100 µm by bar coating). The inset shows 900–1,200 cm^{-1}, which contains IR peaks 1,020–1,074 cm^{-1} (Si-O-Si stretching)[30].

Fabrication and characterization of ASC spheroid–hydrogel composite encapsulated by the nanosheet

Based on the engineering of intrinsically semi-permeable PDMS nanosheets, we designed a cell encapsulation device by compositing ASC spheroids with photo-crosslinked hydrogel (gelatin methacrylate: GelMA) and encapsulated the ASC–GelMA composite within the PDMS nanosheet (Fig. 2a-e).

First, PDMS nanosheets were fabricated by the gravure coating method, which allows for minimizing the film thickness while continuously manufacturing the film at a large scale[19]. We obtained nano- and micrometer-thick PDMS sheets (600 nm and 2.4 µm by gravure coating and 4.8 µm and 100 µm by bar coating) without punctured holes, which was confirmed by scanning electron microscopy (SEM) imaging (Fig. 2f). The Fourier-transform infrared spectroscopy (FTIR) spectra of the PDMS nanosheets showed an Si-O-Si peak at 1,020–1,074 cm^{-1} (Fig. 2g), which indicated the crosslinked structure of PDMS, as previously reported[19,25]. According to the previous report, it can be suggested that the ratio of monomer to crosslinker does not affect the crosslinking density[19]. Given that the absorbance peak of the alkyl group at 2,900 cm^{-1} was nearly the same among the different PDMS nanosheets, a decreased film thickness resulted in a decreased Si-O-Si bond absorbance peak, which suggests a decrease in crosslinking density[19].

The mechanical properties of each device component (i.e., the PDMS nanosheet and GelMA) were evaluated by a tensile test and compression test, respectively, and compared with the mechanical properties of the subcutaneous tissue in which the device would be transplanted (Table 1). The Young's modulus values of the PDMS sheet, regardless of thickness (2 µm and 100 µm), under wet and dry conditions were equivalent (Fig. S1). Therefore, the mechanical properties of the crosslinked structure would not be affected by the implantable conditions *in vivo*. Furthermore, Young's modulus of GelMA, which constitutes the majority of the device, was measured to be 2.8 kPa, which is much lower than that of skin (5 kPa-140 MPa) [26], suggesting that the device would exert low mechanical stress with conformability to the biological tissue (Table 1).

Next, we fabricated the cell encapsulation device in three steps using the PDMS nanosheet. First, a donut-shaped frame (diameter: 10 mm) made of GelMA was placed on PDMS sheets with thicknesses of 2–10 µm (2 cm x 2 cm) (Fig. 2a). Second, a suspension of ASC spheroids in a GelMA solution (30 µL) was injected into the donut hole (Fig. 2b). Finally, another piece of PDMS nanosheet with a thickness of 600 nm was overlaid on the crosslinked ASC/GelMA (Fig. 2c), and excess PDMS nanosheet was removed (Fig. 2d), resulting in the isolation of ASC spheroids within the device (Fig. 2e).

Table 1. Young's moduli of PDMS sheet (2 µm thick prepared by bar coating), GelMA, and skin[26].

PDMS sheet (Tensile test)	GelMA (Compression test)	Skin
5.5 MPa	2.8 kPa	5 kPa–140 MPa

Evaluation of protein permeability through the PDMS nanosheet

We evaluated the permeability of proteins through PDMS nanosheets with different thicknesses (600 nm, 2.4 µm, and 4.8 µm) and the effect of the thickness on the protein-releasing capability. The PDMS nanosheets were attached to the cell culture inserts (Transwell®) in individual wells of a 24-well microplate. Bovine serum albumin (BSA) (molecular weight: 66.5 kDa[16]) was used as a model protein because it has a molecular weight similar to VEGF (45 kDa[27]). Then, the BSA solution was added to the inner part of the Transwell, and the PBS solution (without BSA) was added to the outer part. The plate was read in a multilabel plate reader for up to 24 h to evaluate the time course of the cumulative release of BSA from the inner to the outer well through the PDMS nanosheets. We found that a thinner PDMS nanosheet resulted in a faster permeation speed (Fig. 3a). We evaluated the molecular permeability of BSA through the PDMS nanosheet as a function of cumulative release (%) from the inner part to the outer part of the well using Eq. 1[16]

$$[\boldsymbol{Cumulative\ release}] = \frac{[\boldsymbol{C_t}\ (\boldsymbol{mM})]}{[\boldsymbol{C_\infty}\ (\boldsymbol{mM})]} \times (\mathbf{1})$$

where C_t is the concentration of permeated molecules in the outer well at time t and C_∞ is the concentration of the permeated molecules in the outer well at infinite time ∞. We then calculated the flux of the PDMS nanosheet. The flux was calculated from an initial gradient of the permeation curve using Eq. 2[16]

$$\left[\boldsymbol{Flux}\ (\boldsymbol{mmol\ h^{-1}\ m^{-2}})\right] = \frac{[\boldsymbol{N_t}(\boldsymbol{mmol})]}{[\boldsymbol{t}(\boldsymbol{h}) \times \boldsymbol{A}(\boldsymbol{m^2})]} (\mathbf{2})$$

where N_t is the number of permeated molecules in the outer well at time t (0.5 h), and A is the total area of the transmembrane pores. The value increased markedly as the sheet thickness decreased to 600 nm (Fig. 3b). This result implied that we could control the permeability by changing the thickness of the PDMS nanosheet. Notably, the thinnest PDMS nanosheets that we fabricated had a thickness of 300 nm. However, the release from these sheets was too fast, which would be attributed to the effects of the macroscopic defects (Fig. S2). Therefore, we used the 600 nm-thick PDMS nanosheets to fabricate the cell encapsulation device.

To discuss the permeation mechanism of high molecular weight molecules through the PDMS nanosheet, we will focus on the IR spectra of the PDMS nanosheets with different thicknesses (Fig. 2g). The magnified IR spectrum (Fig. 2g, inset) shows the peaks at 1,020–1,074 cm^{-1}, indicating the presence of Si-O-Si, which is related to the crosslinking degree[19]. The 100 µm- and 2 µm-thick nanosheets fabricated by the bar coater without diluting the PDMS precursor showed almost the same peak intensities, followed by the 2.4 µm and 600 nm nanosheets, both of which were fabricated by gravure coating and diluting the PDMS precursor. These results suggest that the degree of Si-O-Si crosslinking decreased as a result of diluting the

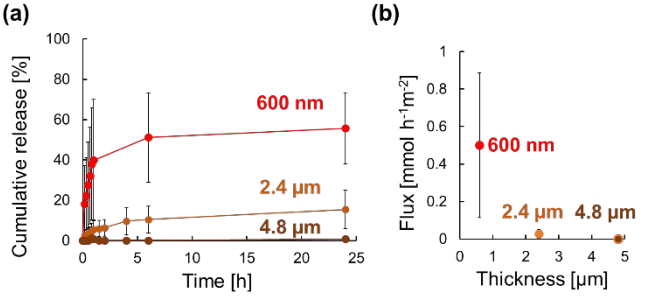

Fig. 3 Permeability of PDMS nanosheets. (a) Time-course study of the cumulative release of BSA through PDMS nanosheets with different thicknesses (red: 600 nm, light brown: 2.4 µm, brown: 4.8 µm), and (b) corresponding relationship between the nanosheet thickness and flux.

PDMS precursor and producing a thinner sheet. The low crosslinking density due to PDMS precursor dilution would allow for the permeation of molecules with large molecular weights such as BSA and VEGF.

Although PDMS is a hydrophobic polymer and permeates organic solvents, a recent study in molecular dynamics simulations showed that ethanol and water molecules can diffuse in PDMS chains[28]. In addition, another study reported atomic force microscopy (AFM) images of PDMS taken using peak force quantitative nanomechanical mapping (PF-QNM) mode; these images showed microporous structures of the surface and inside of cured PDMS with a pore size of 10–16 nm[29]. Another study also reported high-resolution peak force tapping AFM images which showed PDMS surface with porous structure with 14.4 nm mean diameter[30]. Although the curing conditions and sample geometry are different in our study, it is possible that the PDMS nanosheets used in our study may have a similar structure. Another experiment was conducted to evaluate the permeation behavior of different molecular weight through PDMS nanosheet with same thickness. We compared BSA (66.5 kDa) and IgG (150 kDa), which would be interdicted to avoid foreign body reaction. It appears that there may be differences in permeation rate / behavior, but there is no significant difference (Fig. S3). The similarity in the permeability of the two molecules can be assumed to be due to the fact that the size of both molecules are around single-digit nm[31,32].By controlling the thickness and the curing rate of PDMS, IgG might be selectively interdicted.

VEGF release from the cell encapsulation device

We compared the amount of VEGF secreted from ASC spheroids (1,000 spheroids, 5 x 10^5 cells in total) and freely dissociated ASCs (5 x 10^5 cells) by ELISA to ascertain which types of cellular organization would be suitable for the implantable application. The amount of VEGF secreted from ASC spheroids suspended in GelMA with crosslinking was 3.6-times higher than that of the dissociated ASCs in GelMA without crosslinking (Fig. 4a). We recently reported a comparison of VEGF gene expression in ASC spheroids and two-dimensionally adherent ASCs, and the ASC spheroids showed higher VEGF gene expression[33], which is considered to be due to the close interaction of among cells in the microenvironment of spheroid[34]. Based on these results, we concluded that the ASC spheroids with higher VEGF-releasing capability were more suitable than dissociated ASCs for further application.

To evaluate VEGF release from the device, the metabolic activity and amount of VEGF secreted from the ASC spheroids (1,000 spheroids, 5 x 10^5 cells in total) were evaluated. Since it is assumed that a permeable membrane that suppresses foreign body reactions will be used for future allogeneic transplantation, following experiments were conducted here in the form of a device using the membrane. The fluorescence image of the encapsulated ASC spheroids stained with calcein-AM using the Live/Dead Cell Staining Kit indicated that the cells are still alive after 5 days of culturing in medium (Fig. 4b). This means that a minimum amount of nutrients permeated through the PDMS membrane, even if molecular permeability was somewhat suppressed to about 60%. Owing to the continuous viability of the ASC spheroids, we observed an incremental release of VEGF from the cell encapsulation device over 5 days (Fig. 4c). This result suggests that VEGF was continuously released from the ASC spheroids and permeated (VEGF molecular weight: 45 kDa[27]) through the PDMS nanosheet for 5 days. The amount of VEGF released from the cell encapsulation device in Fig. 4c was lower than that released from the non-encapsulated ASC spheroids in Fig. 4a. Such a difference was occurred since the ASC spheroids in the cell encapsulation device were isolated from the surrounding culture medium by the PDMS nanosheet and crosslinked GelMA, which acted as a physical obstacle, resulting in the slower release of VEGF. However, the ability of the cell encapsulation device to continuously release VEGF over several days would be ideal for preconditioning the vascularization process in skin transplantation patients[35] or in diabetic patients who require islet transplantation.

Angiogenic effect of the cell encapsulation device

To evaluate the clinical applicability of the cell encapsulation device, we implanted the ASC spheroid encapsulation device and evaluated the angiogenic effect triggered by the secreted VEGF. The device was transplanted subcutaneously into the right flank region of the dorsal side. The PDMS nanosheet side of the device faced the fascia to investigate the device's angiogenic effect on the subcutaneous layer (Fig. 5a). We confirmed the stable transplantation process by employing a blank device (Fig. 5b), in which the GelMA was stained with Brilliant blue FDF for visualization. Then, the cell encapsulation device was placed in the same position

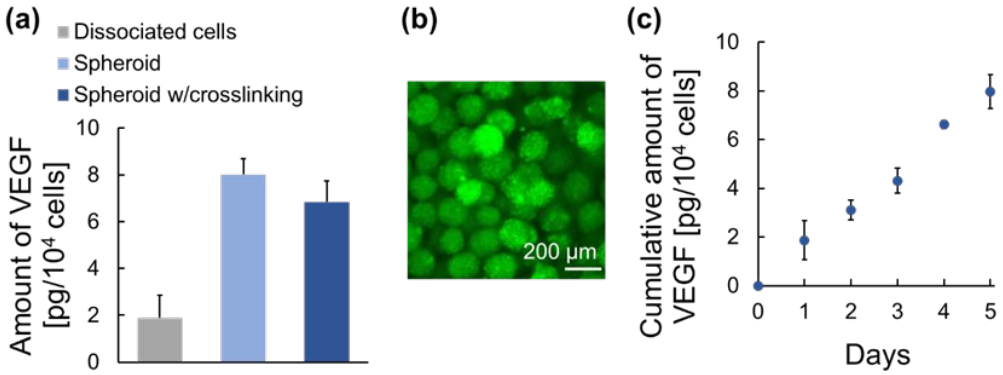

Fig. 4 VEGF released from the cell encapsulation device. (a) Amount of VEGF secreted by dissociated ASCs and ASC spheroids suspended in GelMA without crosslinking after 1 day of culturing. (b) Fluorescent image of ASC spheroids encapsulated in the device after 5 days of culturing, stained with calcein-AM. (c) Cumulative amount of VEGF released from the cell encapsulation device.

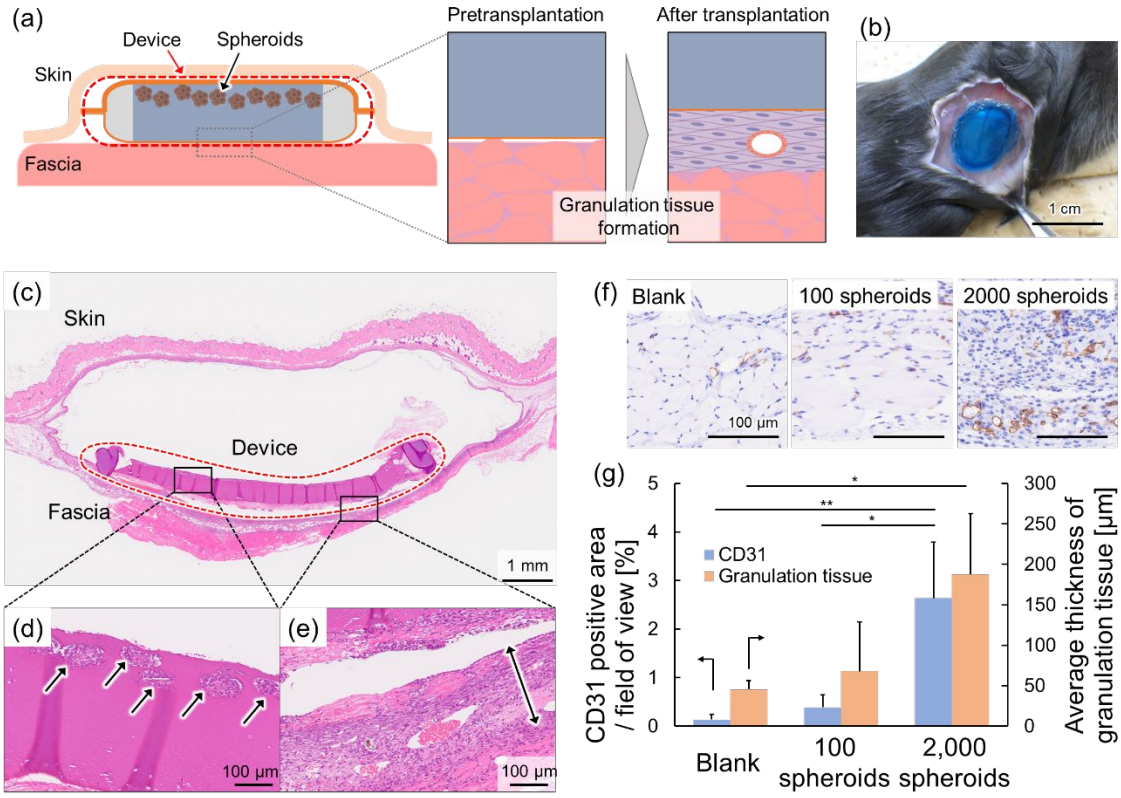

Fig. 5 Angiogenic effect of the cell encapsulation device. (a) Schematic image of the cross-section of the device and tissue around the device before and after transplantation. (b) Optical image of the device transplanted into the subcutaneous area. The device was stained for visualization. (c-e) Histological images of (c) the 2,000 spheroids device sandwiched between skin and fascia at 7 days after transplantation, (d) encapsulated spheroids, and (e) formed granulation tissue. (f) Histological image of blood vessels generated in the granulation tissue. (g) Histological analysis of the CD31-positive area/field of view and average thickness of the granulation tissue formed on the fascia side in contact with the device containing 0 (blank), 100 and 2,000 spheroids. Statistical analysis was performed using Bonferroni's multiple comparison test. (n=5, *$p < 0.05$, **$p < 0.01$)

and covered with skin for implantation for evaluating the angiogenic effect.

Devices encapsulating different amounts of ASC spheroids (0, 100, and 2,000) were subcutaneously transplanted, and the angiogenic effect was evaluated (Table S1). The number of cells in each device was established based on the results shown in Fig. 4, and also considering our previous research[22]. A device sandwiched between the skin and fascia was histologically observed 7 days after transplantation (Fig. 5c), and encapsulated ASC spheroids were observed in the device area (Fig. 5d). In addition, granulation tissue had formed on the fascia of the groups that received 2,000 spheroids (Fig. 5e) and 100 spheroids (Fig. S4a). In contrast, the blank group and the sham group showed the same amount of granulation tissue formation (Fig. S4b, c), suggesting that there was little reaction to the foreign polymeric materials (i.e., PDMS and GelMA). The angiogenic effect of the device was further evaluated by analyzing the hematoxylin & eosin (HE) staining and CD31 immunostaining histological images (Fig. 5f). Compared with the blank group, the 2,000 spheroids group showed 4.1 times greater granulation tissue formation and 19 times greater angiogenic effect (Fig. 5g). Furthermore, the 2,000 spheroids group showed 6.8 times greater angiogenic effect than the 100 spheroids group. These results indicate that the subcutaneous application of the spheroid encapsulation device in mice enhanced the formation of granulation tissue and angiogenesis by secreting VEGF through the PDMS nanosheet. Furthermore, the formation of vascular-rich granulation tissue in the 2,000 spheroids group suggested that increasing the number of spheroids to this level led to the development of an environment suitable for the vascular beds needed for cell transplantation.

The results of this study are limited to the understanding of the physiological contribution of ASC spheroids to angiogenesis *in vivo*. Thus, further optimization of the spheroid number and the thickness of the PDMS nanosheet is required prior to clinical application, such as in diabetic patients, because little is empirically known about the therapeutic efficacy of long-term VEGF release in clinical practice[12,36]. Therefore, it will be important to investigate the usefulness of the cell encapsulation device by comparing it with conventional therapeutics such as the local delivery of growth factors. In addition, although prolonged bioactivity of the implanted cell encapsulation device could be ideal for treatment, a convenient method for refilling ASC spheroids into the implanted device should be developed, for example, by inserting an external tube into the device. It would also be interesting to encapsulate other therapeutic cells (such as islet cells) along with ASC spheroids in the device for the treatment of diabetes and to promote angiogenesis to deliver insulin[14].

4 Conclusions

We developed the ASC spheroid encapsulation device to enable pre-vascularization of the subcutaneous area for cell transplantation therapy. The cell encapsulation device consists

of an intrinsically semi-permeable PDMS nanosheet and microfabricated GelMA. The fabricated device allowed the selective permeability of VEGF with a good conformability to the biological tissue. Notably, we found that the dilution of the precursor PDMS solution led to a low degree of crosslinking density in the PDMS nanosheet, generating an intrinsic protein permeability. The resulting cell encapsulation device continuously released VEGF for 5 days owing to the encapsulated ASC spheroids. Furthermore, the subcutaneously implanted device showed an enhanced angiogenic effect, which potentially suggests the applicability of the device for vascularization in preconditioning purpose in cell transplantation therapy. By controlling the biodegradability of the materials, the device might be applied for differentiation[37]. In addition, further investigation of the permeation mechanism of the nanosheet is expected to improve the efficacy of the cell encapsulation device by optimizing the microstructure including constituent polymers.

Author Contributions

M.T., H.F., and N.Z. performed the experiments and analysed the results. M.T. and H.F. wrote the manuscript under the supervision of H.N., R.A., T.K., and T.F., who also supervised the whole project. Present address of H.F.: Department of Bioengineering, Stanford University, Stanford, CA 94305 (USA).

Conflicts of interest

There are no conflicts to declare.

Acknowledgements

This work was supported by JSPS KAKENHI (grant numbers 18H05469, 21H03815), Ministry of Education, Culture, Sports, Science and Technology (MEXT) Japan, and Fusion Oriented REsearch for Disruptive Science and Technology, Japan Science and Technology Agency (grant number JPMJFR203Q). T.F. is supported by the Leading Initiative for Excellent Young Researchers from MEXT, Japan. H.F. is supported by a Funai Overseas Scholarship, JSPS Doctoral Fellowship (grant number 22J23773), and the Tokyo Tech Academy for Super Smart Society administered by MEXT, Japan.

M.T. and T.F. thank Dr. Yosuke Mizuno for discussions about their histological analysis. The authors also thank Katherine Thieltges from Edanz (https://jp.edanz.com/ac) for editing a draft of this manuscript.

References

1 J. Su, B.-H. Hu, W. L. Lowe Jr, D. B. Kaufman and P. B. Messersmith, *Biomaterials*, 2010, **31**, 308–314.

2 D. An, Y. Ji, A. Chiu, Y.-C. Lu, W. Song, L. Zhai, L. Qi, D. Luo and M. Ma, *Biomaterials*, 2015, **37**, 40–48.

3 A. S. Mao, J.-W. Shin, S. Utech, H. Wang, O. Uzun, W. Li, M. Cooper, Y. Hu, L. Zhang, D. A. Weitz and D. J. Mooney, *Nat. Mater.*, 2017, **16**, 236–243.

4 D. An, A. Chiu, J. A. Flanders, W. Song, D. Shou, Y.-C. Lu, L. G. Grunnet, L. Winkel, C. Ingvorsen, N. S. Christophersen, J. J. Fels, F. W. Sand, Y. Ji, L. Qi, Y. Pardo, D. Luo, M. Silberstein, J. Fan and M. Ma, *Proc. Natl. Acad. Sci. U. S. A.*, 2018, **115**, E263–E272.

5 F. Ozawa, S. Nagata, H. Oda, S. G. Yabe, H. Okochi and S. Takeuchi, *iScience*, 2021, **24**, 102309.

6 W. Liu, Y. Wang, J. Wang, O. L. Lanier, M. E. Wechsler, N. A. Peppas and Z. Gu, *Proc. Est. Acad. Sci. Eng.*, 2022, **13**, 53–70.

7 J. D. Weaver, D. M. Headen, M. D. Hunckler, M. M. Coronel, C. L. Stabler and A. J. García, *Biomaterials*, 2018, **172**, 54–65.

8 S. S. Uematsu, A. Inagaki, Y. Nakamura, T. Imura, Y. Igarashi, I. Fathi, S. Miyagi, N. Ohuchi, S. Satomi and M. Goto, *Transplantation*, 2018, **102**, 387–395.

9 K. Tatarkiewicz, J. Hollister-Lock, R. R. Quickel, C. K. Colton, S. Bonner-Weir and G. C. Weir, *Transplantation*, 1999, **67**, 665–671.

10 A. R. Pepper, B. Gala-Lopez, R. Pawlick, S. Merani, T. Kin and A. M. J. Shapiro, *Nat. Biotechnol.*, 2015, **33**, 518–523.

11 H. Komatsu, D. Kang, H. Lin, C. A. Cook, D. Mendez, J. Rawson, Y. Mullen, F. Kandeel and Y.-C. Tai, *Micro Nano Lett.*, 2016, **11**, 632–635.

12 N. M. Luan and H. Iwata, *Am. J. Transplant*, 2014, **14**, 1533–1542.

13 A. J. Vegas, O. Veiseh, M. Gürtler, J. R. Millman, F. W. Pagliuca, A. R. Bader, J. C. Doloff, J. Li, M. Chen, K. Olejnik, H. H. Tam, S. Jhunjhunwala, E. Langan, S. Aresta-Dasilva, S. Gandham, J. J. McGarrigle, M. A. Bochenek, J. Hollister-Lock, J. Oberholzer, D. L. Greiner, G. C. Weir, D. A. Melton, R. Langer and D. G. Anderson, *Nat. Med.*, 2016, **22**, 306–311.

14 D. T. Bowers, W. Song, L.-H. Wang and M. Ma, *Acta Biomater.*, 2019, **95**, 131–151.

15 S. Bose, L. R. Volpatti, D. Thiono, V. Yesilyurt, C. McGladrigan, Y. Tang, A. Facklam, A. Wang, S. Jhunjhunwala, O. Veiseh, J. Hollister-Lock, C. Bhattacharya, G. C. Weir, D. L. Greiner, R. Langer and D. G. Anderson, *Nat. Biomed Eng*, 2020, **4**, 814–826.

16 T. Fujie, Y. Kawamoto, H. Haniuda, A. Saito, K. Kabata, Y. Honda, E. Ohmori, T. Asahi and S. Takeoka, *Macromolecules*, 2013, **46**, 395–402.

17 S. D. Sheridan, S. Gil, M. Wilgo and A. Pitt, *Methods Cell Biol.*, 2008, **86**, 29–57.

18 M. Mireles and T. R. Gaborski, *Electrophoresis*, 2017, **38**, 2374–2388.

19 K. Yamagishi, I. Kirino, I. Takahashi, H. Amano, S. Takeoka, Y. Morimoto and T. Fujie, *Nat. Biomed Eng*, 2019, **3**, 27–36.

20 S. J. Segal, *Stud. Fam. Plann.*, 1983, **14**, 159–163.

21 D. Shoupe and D. R. Mishell, *Am. J. Obstet. Gynecol.*, 1989, **160**, 1286–1292.

22 Y. Suematsu, H. Nagano, T. Kiyosawa, S. Takeoka and T. Fujie, *J. Biomed. Mater. Res. B Appl. Biomater.*, 2021, **10**, 1245–1254.

23 H. Nagano, Y. Suematsu, M. Takuma, S. Aoki, A. Satoh, E. Takayama, M. Kinoshita, Y. Morimoto, S. Takeoka, T. Fujie and T. Kiyosawa, *Sci. Rep.*, 2021, **11**, 14500.
24 J. Yu, Y.-C. Hsu, J.-K. Lee and N.-C. Cheng, *Stem Cell Res. Ther.*, 2022, **13**, 276.
25 L. M. Johnson, L. Gao, C. W. Shields IV, M. Smith, K. Efimenko, K. Cushing, J. Genzer and G. P. López, *J. Nanobiotechnology*, 2013, **11**, 22.
26 S. Liu, Y. Rao, H. Jang, P. Tan and N. Lu, *Matter*, 2022, **5**, 1104–1136.
27 K. A. Houck, D. W. Leung, A. M. Rowland, J. Winer and N. Ferrara, *J. Biol. Chem.*, 1992, **267**, 26031–26037.
28 A. Ahmad, S.-H. Li and Z.-P. Zhao, *J. Memb. Sci.*, 2021, **620**, 118863.
29 V. Drebezghova, H. Gojzewski, A. Allal, M. A. Hempenius, C. Nardin and G. J. Vancso, *Macromol. Chem. Phys.*, 2020, 2000170.
30 J. A. Goodchild, D. L. Walsh, H. Laurent and S. D. Connell, *Langmuir*, 2023, **39**, 10843–10854.
31 F. L. González Flecha and V. Levi, *Biochem. Mol. Biol. Educ.*, 2003, **31**, 319–322.
32 L. F. Pease 3rd, J. T. Elliott, D.-H. Tsai, M. R. Zachariah and M. J. Tarlov, *Biotechnol. Bioeng.*, 2008, **101**, 1214–1222.
33 Y. Suematsu, Y. A. Tsai, S. Takeoka, C. M. Franz, S. Arai and T. Fujie, *J. Mater. Chem. B Mater. Biol. Med.*, 2020, **8**, 6999–7008.
34 N.-C. Cheng, S. Wang and T.-H. Young, *Biomaterials*, 2012, **33**, 1748–1758.
35 A. Ferretti, E. Boschi, A. Stefani, S. Spiga, M. Romanelli, M. Lemmi, A. Giovannetti, B. Longoni and F. Mosca, *Life Sci.*, 2003, **73**, 1985–1994.
36 R. E. Levey, F. B. Coulter, K. C. Scheiner, S. Deotti, S. T. Robinson, L. McDonough, T. T. Nguyen, R. Steendam, M. Canney, R. Wylie, L. P. Burke, E. B. Dolan, P. Dockery, H. M. Kelly, G. Ghersi, W. E. Hennink, R. J. Kok, E. O'Cearbhaill and G. P. Duffy, *Pharmaceutics*, 2021, **13**, 2077.
37 E. E. Huang, N. Zhang, E. A. Ganio, H. Shen, X. Li, M. Ueno, T. Utsunomiya, M. Maruyama, Q. Gao, N. Su, Z. Yao, F. Yang, B. Gaudillière and S. B. Goodman, *J Orthop Translat*, 2022, **36**, 64–74.